5482 *Biochemistry* **2010,** *49,* 5482–5493
DOI: 10.1021/bi100631f

BIOCHEMISTRY
including biophysical chemistry & molecular biology
Article

Membrane Association Facilitates Degradation and Cleavage of the Cyclin-Dependent Kinase 5 Activators p35 and p39[†]

Seiji Minegishi,* Akiko Asada, Shinya Miyauchi, Takahiro Fuchigami, Taro Saito, and Shin-ichi Hisanaga*

Department of Biological Sciences, Graduate School of Science, Tokyo Metropolitan University, Minami-Osawa 1-1, Hachioji, Tokyo 192-0397, Japan

Received April 26, 2010; Revised Manuscript Received June 2, 2010

ABSTRACT: Cyclin-dependent kinase 5 (Cdk5) is activated by binding to its activators, p35 and p39. The level of Cdk5 activity is determined by the amount of p35 and p39, which is regulated not only by transcription but also via proteasomal degradation. Alternatively, calpain-induced cleavage of p35 to p25 can induce aberrant Cdk5 activation. As the regulation of p35 and p39 proteolysis is not well understood, we have studied here the mechanisms governing their degradation and cleavage. We find that p35 and p39 undergo proteasomal degradation in neurons, with p39 showing a slower degradation rate than p35. Degradation of the activators is dependent on their respective N-terminal p10 region, as indicated by experiments in which cognate p10 regions were swapped between p35 and p39. The effect of the p10 region on degradation and cleavage could be assigned to its membrane binding properties, mediated predominantly by myristoylation. Together, these results indicate that both proteasomal degradation and calpain cleavage of p35 and p39 are stimulated by membrane association, which is in turn mediated via myristoylation of their p10 regions. However, p35 and p39 show differences in degradation and cleavage rates, which may in fact underlie the distinct physiological and pathological functions of these two Cdk5 activators.

Cyclin-dependent kinase 5 (Cdk5)[1] is predominantly expressed in postmitotic neurons and has been implicated in brain development, synaptic plasticity, and neurodegeneration (*1*−*4*). Cdk5 is activated by binding to its activators, p35 and p39, which are strongly expressed in neurons (*5*, *6*). In fact, the available amount of p35 and p39 determines the kinase activity of Cdk5 (*6*, *7*). The protein level of p35 and p39 can be regulated by de novo synthesis as well as degradation. Proteasomal degradation of p35 has been found to be a major mode of regulation of Cdk5 activity (*8*−*10*); thus, a similar mechanism is predicted for p39. It is well established that degradation of cyclins in proliferating cells is essential for cell cycle progression (*11*). Likewise, degradation of Cdk5 activators is likely to play an important role in regulating neuronal functions. In support of this notion, treatment of cortical neurons with the excitatory neurotransmitter glutamate triggers degradation of p35, subsequently resulting in transient inactivation of Cdk5 (*12*, *13*). Thus, physiological functions of Cdk5 are governed via the degradation of activator proteins, thereby reducing Cdk5 activators. However, neither the degradation mechanism nor the degradation machinery for p35 or p39 is well understood.

The Cdk5 activators are composed of two domains, the N-terminal cell localization targeting domain and the C-terminal Cdk5 activation domain. The N-terminal region, p10, includes the N-myristoylation consensus sequence MGXXXS/T (*14*, *15*). Myristoylation at this site confers membranal localization to p35 and p39 (*16*). The C-terminal domains assume a globular conformation and are highly homologous (70% identical) (*17*). Interaction of Cdk5 with either C-terminal domain is sufficient for activation, but their binding affinity varies, with p39 showing a lower affinity for Cdk5 than p35 (*18*). Neurotoxic stimuli have been found to induce cleavage of p35 and p39 by calpain, a calcium-dependent protease, generating p25 and p29, respectively (*10*, *15*, *19*, *20*). Formation of p25 induces abnormal activation of Cdk5, first by prolonging Cdk5 activation through the longer half-life of p25 compared to that of p35 (*15*, *20*) and second through liberation of the kinase from its otherwise membrane-restricted localization, allowing it access to a different set of substrates (*15*, *21*). In addition, the release of the p25−Cdk5 complex liberates the complex from the inhibitory action that membranes have on the kinase activity of the p35−Cdk5 complex (*22*). Thus, p25 confers increased Cdk5 activity toward abnormal substrates and as such has been implicated in neuronal cell death. In contrast, functional consequences of cleavage of p39 to p29 are not yet known. To date, the cleavage of p35 and p39 has been studied separately (*9*, *10*), and thus, their cleavage properties have not been compared.

Knockout mouse studies show that the active kinase complexes, p35−Cdk5 and p39−Cdk5, have distinct but overlapping functions. Mice lacking p35 display an inverted neuronal lamination pattern in the cerebral cortex, but mice lacking p39 do not show an abnormal phenotype (*23*, *24*). However, mice lacking both p35 and p39 exhibit abnormal lamination patterns in various brain regions and die soon after birth, resembling those of mice lacking Cdk5 (*24*, *25*). These results indicate that developmental neuronal functions of Cdk5 are mainly mediated

[†]This work was supported part by Grants-in-Aid for Scientific Research on Priority Area from MEXT of Japan.

*To whom correspondence should be addressed: Minami-Osawa 1-1, Hachioji, Tokyo 192-0397, Japan. Telephone: +81-42-677-2769. Fax: +81-42-677-2559. E-mail: minegishi-seiji@ed.tmu.ac.jp or hisanaga-shinichi@tmu.ac.jp.

[1]Abbreviations: AD, Alzheimer's disease; Cdk5, cyclin-dependent kinase 5; CHX, cycloheximide; DIV7, day 7 in vitro; DMEM, Dulbecco's modified Eagle's medium; FBS, fetal bovine serum; PBS, phosphate-buffered saline; MG132, benzyloxycarbonyl-leucyl-leucyl-leucinal; NP-40, Nonidet P-40; SDS, sodium dodecyl sulfate; WT, wild-type.

 Published on Web 06/02/2010

by p35 and p39, and that p35−Cdk5 and p39−Cdk5 have different functions but can partially compensate for each other. So far, most reports have examined p35−Cdk5, and thus, little is known about p39−Cdk5.

In this study, we have focused on the mechanisms regulating the degradation and cleavage of p35 and p39 in neurons. We find that p39 is degraded more slowly than p35 by the proteasomes when protein synthesis is inhibited by cycloheximide (CHX). Furthermore, we have investigated the effect of membrane association on degradation and cleavage of p35 and p39. For this purpose, we have analyzed the degradation rate of p35 and p39 molecules that were mutated at their myristoylation sites, or in which their cognate N-terminal p10 regions have been swapped, and studied p25 and p29 tagged with the N-terminal myristoylation signals. These experiments demonstrate that the p10 region of p35 and p39 determines the proteolytic properties by conferring membrane association and thereby accelerating degradation and cleavage. Differences in the proteasomal degradation and calpain cleavage between p35 and p39 are discussed in relation to their physiological and pathological functions.

MATERIALS AND METHODS

Antibodies and Chemicals. Cycloheximide (CHX) and glutamate were purchased from Sigma (St. Louis, MO); benzyloxycarbonyl-leucyl-leucyl-leucinal (MG132) was purchased from Peptide Institute (Osaka, Japan), and ionomycin and Epoxomicin were obtained from Calbiochem (San Diego, CA). The anti-Cdk5 antibody (DC17) and the anti-p35 antibody (C19) were obtained from Santa Cruz Biotechnology (Santa Cruz, CA). The anti-myc antibody (9E10), anti-Flag antibody, and anti-actin antibody were purchased from Sigma. The anti-myc antibody (4A6) was from Upstate. The anti-p39 antibody (C14) has been described previously (*18*). Protein G Dynabeads were purchased from Invitrogen (Carlsbad, CA). Protein A Sepharose was purchased from GE Healthcare (Buckinghamshire, U.K.). [^{35}S]Methionine was obtained from Institute of Isotopes Co., Ltd. (Budapest, Hungary). ImmunoPure Gentle Ag/Ab Elution Buffer and disuccinimidyl suberate were purchased from Pierce Biotechnology, Inc. (Rockford, IL).

Construction of Mammalian Cell Expression Vectors. pcDNA3 mouse p35 or p39 constructs, pEGFP-N98^{p35}, pEGFP-N100^{p39}, and pcDNA3-HA-Cdk5 have been reported previously (*16*). pcDNA3-p25-myc was constructed by PCR amplification using pcDNA3-p35-myc as a template with 5′-AAGCTTATGCGCGAGAACCTTCTCCGCAAG-3′ and 5′-CGGAATTCTCACAGATCCTCTTCTGAGATGAGTTTTTGTTCCCGATCCAGCCCCAGGA-3′ as forward and reverse primers, respectively. pcDNA3-p29-myc was constructed by PCR amplification using pcDNA3-p39-myc as a template with 5′-AAGCTTATGGCCCAGCCCCCGCCGGCTCAG-3′ and 5′-CGGAATTCTCACAGATCCTCTTCTGAGATGAGTTTTTGTTCGCGGTCCAAGTTCATAG-3′ as forward and reverse primers, respectively. The PCR products were ligated into the pCR2.1 TA cloning vector (Invitrogen) and then transferred into pcDNA3 using *Hin*dIII and *Eco*RI. pcDNA3-N7-p25-myc was constructed by PCR amplification using pcDNA3-p35-myc as a template with 5′-GCCCAGCCCCCGCCGGCTCAG-3′ and 5′-TAGGGACAGCACCGTGCCCAT-3′ as forward and reverse primers, respectively, to omit nucleotides 22−294, corresponding to amino acids 8−98 of p35. pcDNA3-N7-p29-myc was constructed by PCR amplification using pcDNA3-p29-myc as a template with 5′-AAGCTTATGGGCACGGTGCTGTCGCTTCGCGAGAACCTTCTCCGCAAG-3′ as the forward primer; the reverse primer was that used for construction of pcDNA3-p29-myc. pcDNA3-N7 G2A-p25-myc and N7 G2A-p29-myc were constructed by PCR amplification using pcDNA3-N7-p25-myc and N7-p29-myc, respectively, as templates with 5′-CAAGCTTATGGCCACGGTGCTGT-3′ as the forward primer for both reactions; the reverse primers were those used for construction of pcDNA3-p25-myc and p29-myc, respectively. pcDNA3-N100^{p39}-p25-myc was constructed as follows. N100^{p39} with a *Hin*dIII site at the 5′ end and a blunt end at the 3′ end was amplified by PCR using pcDNA3-p39-myc as a template with 5′-AATAAGCTTATGGGCACGGTGCTGTC-3′ as the forward primer and 5′-GTTGCGTTGCTGGACCAGAGGGTCGGGA-3′ as the reverse primer. p25-myc with a blunt end at the 5′ end and an *Eco*RI site at the 3′ end was amplified by PCR using pcDNA3-mouse p35-myc as a template with 5′-GCCCAGCCCCCGCCGGCTCA-3′ as a forward primer and the same reverse primer used for PCR of p25-myc. The PCR products of N100^{p39} and p25-myc were ligated into pcDNA3 at the *Hin*dIII and *Eco*RI sites. pcDNA3-N98^{p35}-p29-myc was constructed as follows. N98^{p35} with a *Hin*dIII site at the 5′ end and a blunt end at the 3′ end was amplified by PCR using pcDNA3-p35-myc as a template with the same forward primer used for N100^{p39} and 5′-GAATGTGGACAGGTTGGCACAGGA-3′ as a reverse primer. p29-myc with a blunt end at the 5′ end and an *Eco*RI site at the 3′ end was amplified by PCR using pcDNA3-p39-myc as a template with 5′-AAGCTTATGGCCCAGCCCCCGCCGGCTCAG-3′ as a forward primer and the same reverse primer used for p29-myc. The PCR products of N98^{p35} and p29-myc were ligated into pcDNA3 at the *Hin*dIII and *Eco*RI sites. All plasmid constructs were verified by DNA sequencing.

Cell Culture and Transfection. HEK293 cells were cultured in Dulbecco's modified Eagle's medium (DMEM, Sigma) containing 10% fetal bovine serum (FBS) and were transfected with p35 or p39 expression plasmids using a PolyFect transfection regent (Qiagen, Valencia, CA). Rat brain cerebellar granule neurons were prepared according to the method described by Tabuchi et al. (*26*). Granule neurons prepared from 7-day-old rat cerebellum were plated at a density of 4.6×10^5 cells/cm^2 in polyethyleneimine-coated dishes in DMEM containing 10% FBS. The medium was changed to Neurobasal (Invitrogen) supplemented with B-27 (Invitrogen) and 1 mM L-glutamine 3 h after plating. Neuron cultures were used on day 7 in vitro (DIV7) or on day 14 in vitro (DIV14). Rat brain cortical neurons were prepared according to the method described by Endo et al. (*27*). Rat brain cortex from embryonic day 17 or 18 was dissected, and neurons were plated as described above in DMEM and Ham's F12 (1:1) containing 5% FBS and 5% horse serum. The medium was then changed to Neurobasal medium supplemented with B-27 and 1 mM L-glutamine (*27*). Cortical neuron cultures were also used on DIV7 or DIV14.

Adenoviral Expression of p35 and p35 G2A in Cultured Neurons. Flag-tagged wild-type human p35 has been reported previously (*28*). Human p35 G2A in pShuttle (Clontech, Palo Alto, CA) was constructed by PCR amplification using pShuttle-p35 G2A-Flag as a template with 5′-TCTAGAATGGCCACGGTGCTGT-3′ and 5′-GGGGTACCTCACTTGTCGTCATCGTCTTTGTAGTCCCGATCCAGGCCTAGG-3′ as forward and reverse primers, respectively. p35 G2A-Flag was ligated into Adeno-X viral DNA (Clontech), and adenoviruses were generated according to the manufacturer's instructions. Cerebellar granule neurons were infected on DIV5 and used on DIV7.

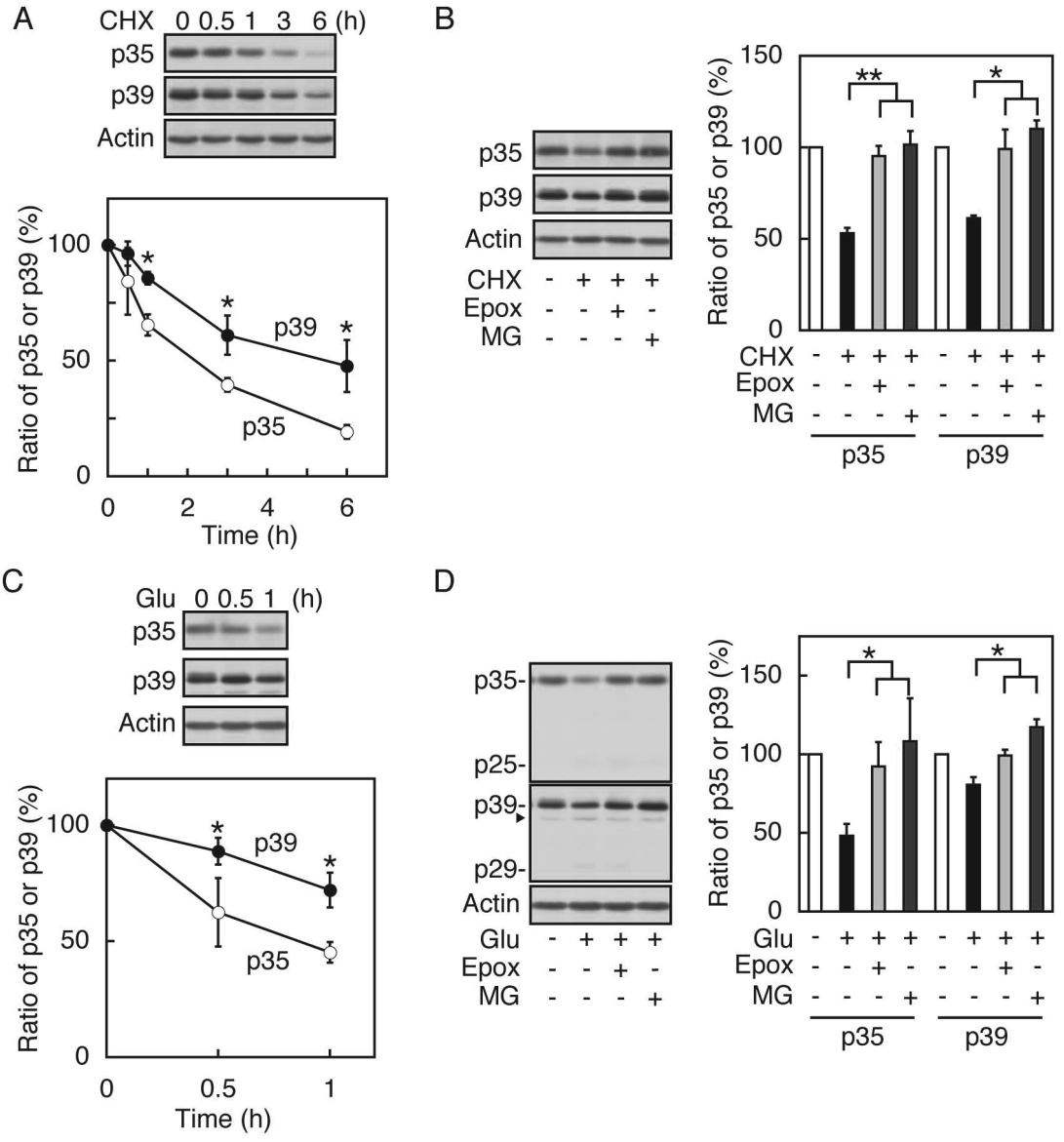

FIGURE 1: p39 is degraded more slowly than p35 by proteasomes in cerebellar granule neurons. (A) Comparison of p35 and p39 degradation in cerebellar granule neurons. Cerebellar granule neurons on DIV7 were treated with 10 μg/mL CHX for the indicated times. p35 and p39 were detected by immunoblotting using anti-p35 and anti-p39 antibodies, respectively (top), and the levels of p35 (○) and p39 (●) were quantified (bottom). Actin was quantified as a loading control. Data represent the means ± the standard error ($n = 3$, $^*p < 0.05$, Student's t test). (B) Degradation of p35 and p39 by proteasomes in cerebellar granule neurons. Cerebellar granule neurons on DIV7 were treated with 10 μM Epoxomicin (Epox) or 20 μM MG132 (MG) in the presence of 10 μg/mL CHX for 3 h. Immunoblotting of p35 and p39 (left) and their quantification (right) are as described above. Data represent the means ± the standard error ($n = 3$, $^{**}p < 0.05$, $^*p < 0.01$, Student's t test). (C) Effect of glutamate on the degradation of p35 and p39 in cerebellar granule neurons. Cerebellar granule neurons on DIV7 were treated with 100 μM glutamate (Glu) for 0.5 and 1 h. Immunoblotting of p35 and p39 (top) and their quantification (bottom) were as described above: (○) p35 and (●) p39. Data represent the means ± the standard error ($n = 3$, $^*p < 0.05$, Student's t test). (D) Glutamate-induced degradation of p35 and p39 by proteasomes in cerebellar granule neurons. Cerebellar granule neurons on DIV7 were treated with 10 μM glutamate (Glu) in the presence of 20 μM Epoxomicin (Epox) or 20 μM MG132 (MG) for 1 h. Immunoblotting of p35 and p39 (left) and their quantification (right) are as described above. The positions of p25 and p29, which are faint, are indicated. The arrowhead in the p39 blot indicates a nonspecific band. Data represent the means ± the standard error ($n = 3$, $^*p < 0.05$, Student's t test).

Pulse−Chase Experiments. HEK293 cells expressing p35-myc, p35 G2A-myc, p39-myc, or p39 G2A-myc and HA-Cdk5 were cultured in methionine-free DMEM supplemented with 100 units/mL penicillin, 0.1 mg/mL streptomycin, 4.07×10^6 Bq/mL [^{35}S]methionine, and 10% FBS that had been previously dialyzed against phosphate-buffered saline (PBS) for 1 h. After being washed twice with PBS, cells were further cultured in DMEM containing 10% FBS. The cells were lysed in RIPA buffer [20 mM Tris-HCl (pH 7.5), 150 mM NaCl, 1 mM EDTA, 0.5 mM EGTA, 1% (w/v) Nonidet P-40 (NP-40), 0.1% sodium dodecyl sulfate (SDS), and 0.1% deoxycholate] containing protease and phosphatase inhibitors (0.2 mM Pefabloc SC, 10 μg/μL leupeptin, 10 mM β-glycerophosphate, 1 μM microcystin-LR, 5 mM NaF, and 1 mM Na_3VO_4). The lysates were diluted with an equal volume of MOPS buffer [20 mM MOPS (pH 7.5), 1 mM $MgCl_2$, 1 mM EDTA, 0.1 mM EGTA, 100 mM NaCl, and 0.5% NP-40] containing protease and phosphatase inhibitors. After centrifugation at 10000g for 20 min, p35 or p39 was immunoprecipitated from the supernatant using anti-p35 (C19)-bound protein G Dynabeads or anti-p39 (C14)-bound protein A Sepharose, respectively. The beads were washed four times with MOPS buffer, and p35 immunoprecipitates were boiled in Laemmli Sample

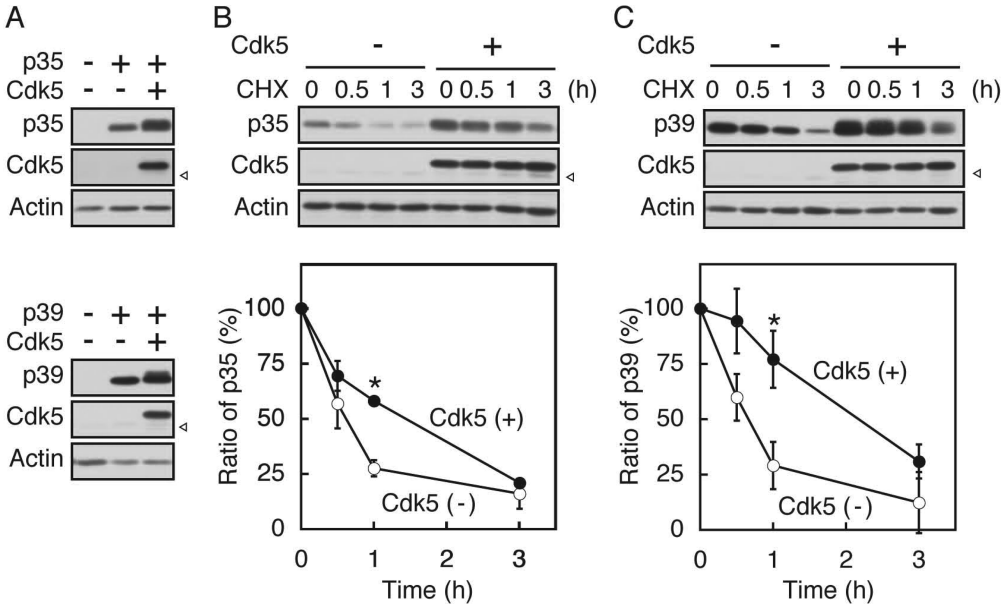

FIGURE 2: Effect of the co-expression of Cdk5 on the stability of p35 and p39. (A) Immunoblot analysis of p35 or p39 expressed with or without Cdk5 in HEK293 cells. p35 (top) and p39 (bottom) were detected using an anti-p35 antibody and an anti-myc antibody (9E10), respectively. Cdk5 levels were detected using an anti-Cdk5 antibody. The position of endogenous Cdk5 is indicated by a white arrowhead. Actin was used as a loading control. (B) Rate of degradation of p35 expressed with or without Cdk5 in HEK293 cells. HEK293 cells expressing p35 in the presence (+) or absence (−) of exogenous Cdk5 were treated with 10 μg/mL CHX for the indicated times. p35 and Cdk5 were detected using anti-p35 and anti-Cdk5 antibodies, respectively. Actin was analyzed as a loading control. Levels of p35 in the absence (○) or presence (●) of Cdk5 were quantified by densitometric analysis (bottom). Data represent the means ± the standard error ($n = 3$, $^*p < 0.05$, Student's t test). (C) Rate of degradation of p39 expressed with or without Cdk5 in HEK293 cells. HEK293 cells expressing p39 in the presence (+) or absence (−) of Cdk5 were treated as described for panel B. p39 and Cdk5 were detected using an anti-myc antibody (9E10) and an anti-Cdk5 antibody, respectively. Levels of p39 in the absence (○) or presence (●) of Cdk5 were quantified by densitometric analysis (bottom). Data represent the means ± the standard error ($n = 3$, $^*p < 0.05$, Student's t test).

Buffer (*18*). p39 immunoprecipitates were eluted with ImmunoPure Gentle Ag/Ab Elution Buffer according to the manufacturer's protocol, concentrated by trichloroacetic acid (TCA) precipitation, and then boiled in Laemmli Sample Buffer. Samples were subjected to 12.5% SDS−PAGE analysis, and proteins were transferred to polyvinylidene difluoride (PVDF) membranes (Millipore, Bedford, MA). [^{35}S]Methionine-labeled p39 and p35 were detected using a FLA7000 image analyzer (Fuji Film, Tokyo, Japan).

SDS−PAGE and Immunoblotting. SDS−PAGE and immunoblotting were performed as described previously (*16*). All experiments were performed at least three times, and representative results are shown in the figures. Data were analyzed using the Student's t test, and a p value of <0.05 was considered to be statistically significant.

RESULTS

The Cdk5 Activator p39 Is More Stable Than p35. Previously, p35 and p39 were found to have a rapid turnover rate (*8*−*10*, *28*). However, their stability has never been compared directly in neuronal cells, and the effect of their mutual presence on degradation has also never previously been analyzed. Thus, we studied the endogenous degradation rates of p35 and p39 in neurons. We used cerebellar granule neurons as our experimental system because both p35 and p39 are expressed in developing cerebellum (*29*). Consistently, we detected p35 as well as p39 in cerebellar granule neurons on DIV7 (Figure 1A). When neurons were treated with the protein synthesis inhibitor cycloheximide (CHX), which is commonly used in degradation experiments, levels of p39 decreased more slowly than levels of p35 (Figure 1A). As p39 and p35 could also be detected in cortical neurons, we performed the same experiments with cortical neurons and obtained similar results (data not shown). As the degradation rate of p39 is slower than that of p35, it raises the question of whether p39 is degraded by proteasomes. When cerebellar granule neurons were treated with CHX for 3 h in the presence of the proteasome inhibitor Epoxomicin or MG132 (Figure 1B), the decrease in the level of p39, as well as p35, was suppressed, indicating that p39 is also degraded by proteasomes.

Degradation of p35 can be induced by glutamate treatment in cortical neuronal cultures (*12*, *13*). Thus, we next examined whether degradation of p39 is also stimulated by glutamate using cerebellar granule neurons. Treatment of cerebellar granule neurons with 100 μM glutamate for 0.5 or 1 h induced p35 degradation. Comparably, levels of p39 decreased, but at a slower rate. The level of p35 was decreased by approximately 55%, whereas p39 levels were decreased by approximately 30% after a 1 h glutamate treatment (Figure 1C). Glutamate-induced degradation of p39 was also shown to be proteasome-dependent by inhibition with Epoxomicin or MG132 (Figure 1D). Under this experimental condition, little formation of p25 and p29 was detected for both p35 and p39 (Figure 1D). Together, these results reveal that p35 and p39 are degraded by the proteasomes, albeit with different degradation rates. Furthermore, proteasomal degradation is consistent with data from all cell systems tested so far, suggesting this is a universally acting mechanism.

Difference in the Degradation of p35 and p39 in HEK293 Cells. To identify the regions within p35 and p39 that affect degradation and to investigate the nature of the difference in degradation rates, we studied the exogenous expression of mutant p35 and p39 species. As the degradation mechanism for p35 and p39 seems to be conserved between proliferating cells

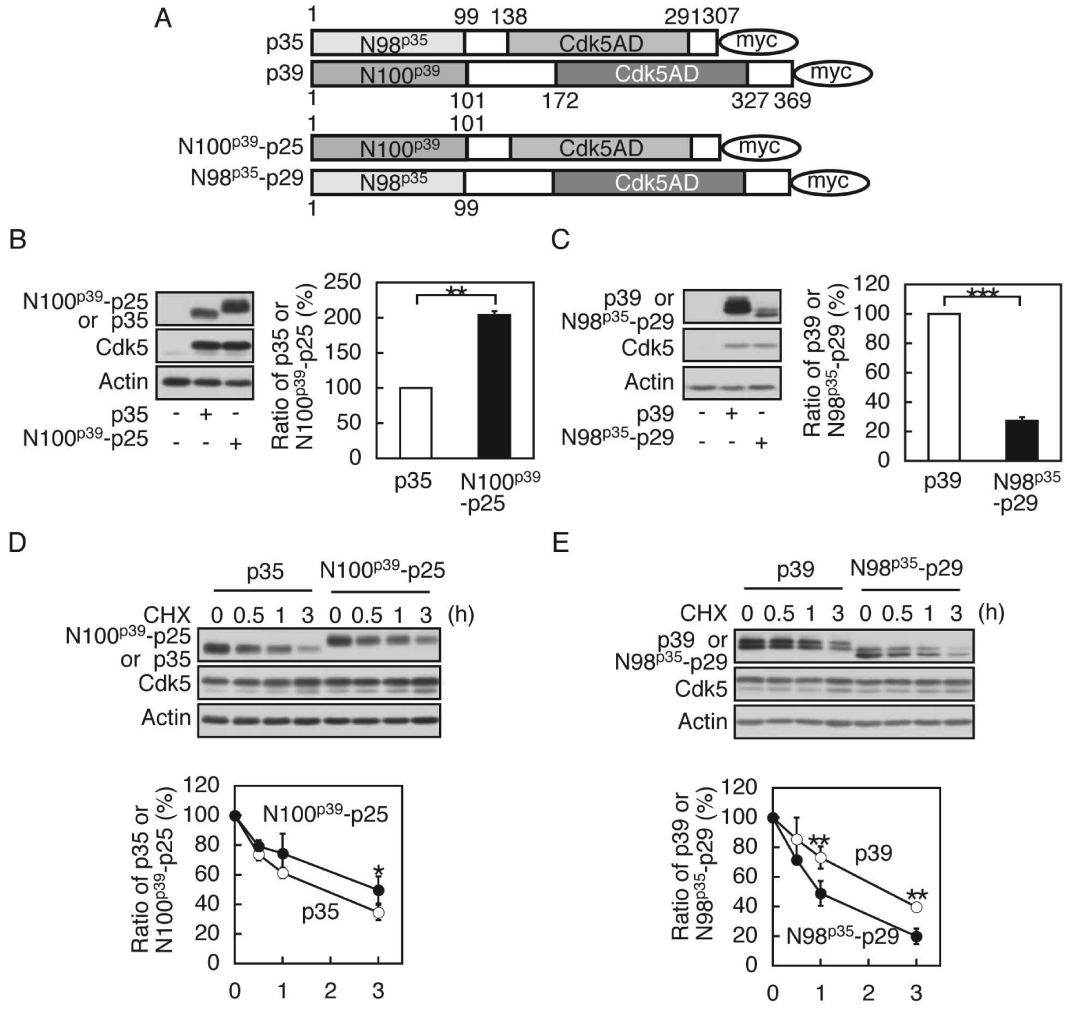

FIGURE 3: Effect of swapping cognate p10 regions between p35 and p39 on their degradation. (A) Schematic representation of p35, p39, and p10 domain-swapped activators, $N100^{p39}$-p25 and $N98^{p35}$-p29. $N100^{p39}$-p25 is a chimeric protein composed of the N-terminal p10 region of p39 and C-terminal p25 of p35. $N98^{p35}$-p29 is a chimeric protein composed of the N-terminal p10 region of p35 and C-terminal p29 of p39. The C-terminal Cdk5 activation domains (Cdk5AD) of p35 and p39 are colored light gray and dark gray, respectively. (B) Expression of p35 or $N100^{p39}$-p25 in HEK293 cells. HEK293 cells were cotransfected with Cdk5 and p35 or $N100^{p39}$-p25 expression plasmids, followed by immunoblot analysis using an anti-p35 antibody to detect p35 and $N100^{p39}$-p25 or an anti-Cdk5 antibody. Actin was analyzed as a loading control. The levels of $N100^{p39}$-p25 relative to that of p35 are quantified in the right panel. Data represent the means ± the standard error ($n = 3$, $^{**}p < 0.01$, Student's t test). (C) Expression of p39 or $N98^{p35}$-p29 in HEK293 cells. HEK293 cells were cotransfected with Cdk5 and p39 or $N98^{p35}$-p29 expression plasmids, followed by immunoblot analysis using an anti-myc antibody (4A6) to detect p39 and $N98^{p35}$-p29 or an anti-Cdk5 antibody. Actin was analyzed as a loading control. The levels of p39 and $N98^{p35}$-p29 are quantified in the right panel. Data represent the means ± the standard error ($n = 3$, $^{***}p < 0.005$, Student's t test). (D) Rate of degradation of p35 or $N100^{p39}$-p25 in HEK293 cells. HEK293 cells co-expressing Cdk5 and p35 or $N100^{p39}$-p25 were treated with 10 μg/mL CHX for the indicated times. Cdk5 and p35 or $N100^{p39}$-p25 were analyzed by immunoblotting (top), and the quantification is shown (bottom). Actin was probed as a loading control: (○) p35 and (●) $N100^{p39}$-p25. Data represent the means ± the standard error ($n = 3$, $^{*}p < 0.05$, Student's t test). (E) Rate of degradation of p39 or $N98^{p35}$-p29 in HEK293 cells. HEK293 cells co-expressing Cdk5 and p39 or $N98^{p35}$-p29 were treated as described for panel D. Cdk5 and p39 or $N98^{p35}$-p29 were analyzed by immunoblotting (top), and the quantification is shown (bottom). Actin was probed as a loading control: (○) p39 and (●) $N98^{p35}$-p29. Data represent the means ± the standard error ($n = 3$, $^{**}p < 0.01$, Student's t test).

and cultured neurons, we used HEK293 cells, as they represent an easily controllable system for overexpression studies. First, we examined the degradation of p35 and p39 in HEK293 cells. When p35 or p39 was transfected with or without Cdk5 in HEK293 cells, expression levels of p35 and p39 were increased by co-expression with Cdk5 (Figure 2A). Their degradation rates were compared in the presence of CHX. Both p35 and p39 were short-lived proteins in HEK293 cells: p35 and p39 were degraded to 27 and 29% with a 1 h CHX treatment, respectively (Figure 2B,C). Co-expression of Cdk5 decreased the degradation rates of both p35 and p39 (Figure 2B,C). A similar result is reported with p35 (*8*).

We proceeded to investigate the effect of the two distinct p10 regions from p35 and p39 on degradation by swapping them on their parent proteins. Thus, chimeric proteins $N100^{p39}$-p25 and $N98^{p35}$-p29 were constructed, as shown in Figure 3A. When they were expressed transiently in HEK293 cells, the protein level of $N100^{p39}$-p25 was 2 times higher than that of full length p35 (Figure 3B), and conversely, that of $N98^{p35}$-p29 was only 25% of that of full length p39 (Figure 3C). The rate of degradation of $N100^{p39}$-p25 and $N98^{p35}$-p29 was estimated in the presence of CHX. The level of $N100^{p39}$-p25 decreased more slowly than the level of wild-type p35 (Figure 3D). In contrast, the level of $N98^{p35}$-p29 decreased faster than the level of wild-type p39 (Figure 3E). Degradation of chimeric proteins was proteasome-dependent as was shown by inhibition with Epoxomicin and MG132 (Figure S1B,C of the Supporting Information). To confirm that these degradation rates are the intrinsic property

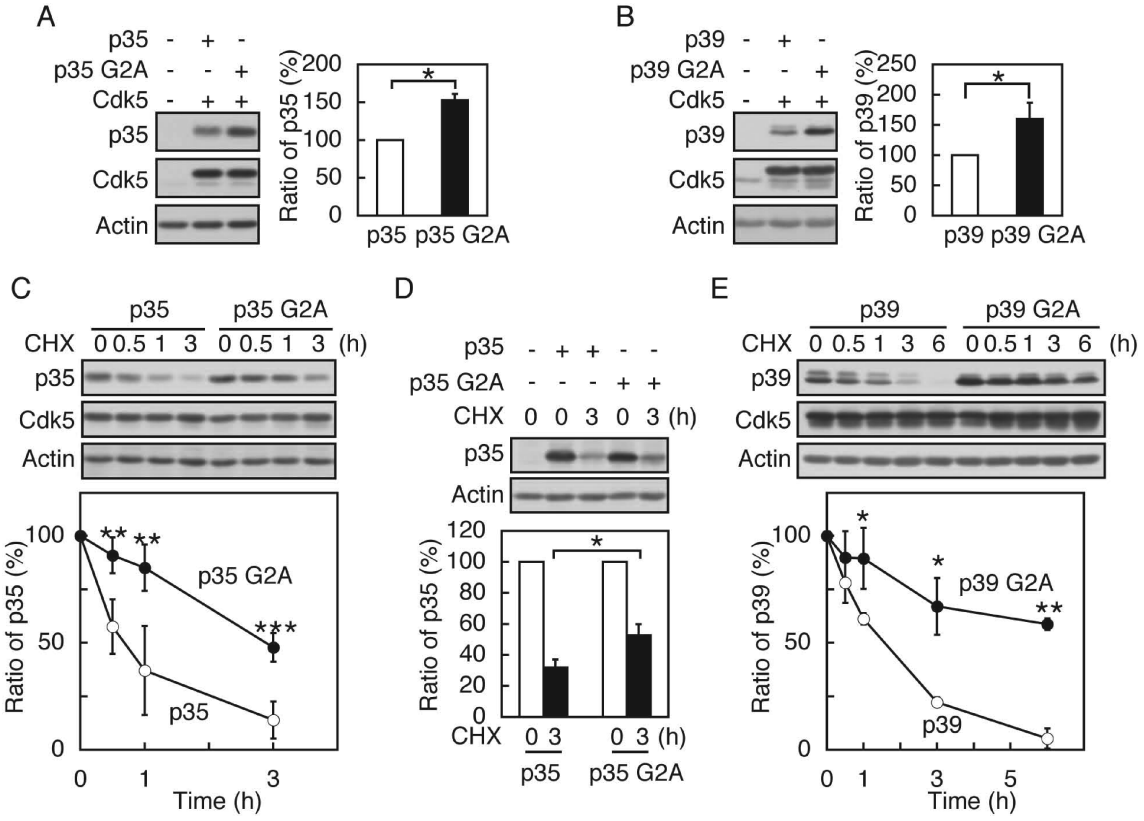

FIGURE 4: Effect of the G2A mutation on the expression of p35 and p39. (A) Expression of p35 or its G2A mutant in HEK293 cells. HEK293 cells were cotransfected with Cdk5 and p35 or p35 G2A expression plasmids for 24 h followed by immunoblot analysis using an anti-p35 antibody to detect p35 constructs or an anti-Cdk5 antibody. Actin was analyzed as a loading control. The levels of p35 G2A relative to that of p35 were quantified [right panel, means ± standard error ($n = 3$, $*p < 0.05$, Student's t test)]. (B) Expression of p39 or its G2A mutant in HEK293 cells. HEK293 cells were cotransfected with Cdk5 and p39 or p39 G2A expression plasmids for 24 h followed by immunoblot analysis using an anti-myc antibody (9E10) to detect p39 constructs or an anti-Cdk5 antibody. The levels of p39 G2A were quantified and expressed as a ratio to p39 [right panel, means ± standard error ($n = 3$, $*p < 0.05$, Student's t test)]. (C) Rate of degradation of p35 and p35 G2A in HEK293 cells. HEK293 cells co-expressing Cdk5 and p35 or p35 G2A were treated with 10 μg/mL CHX for the indicated times. Immunoblots of p35, p35 G2A, and Cdk5 are shown in the top panel, and quantification of p35 and p35 G2A is shown in the bottom panel: (○) p35 and (●) p35 G2A. Data represent the means ± the standard error ($n = 3$, $**p < 0.01$, $***p < 0.001$, Student's t test). (D) Degradation of p35 and p35 G2A exogenously expressed in cerebellar granule neurons. Cerebellar granule neurons infected with adenovirus-p35-Flag or p35 G2A-Flag were treated with 10 μg/mL CHX for 3 h. p35-Flag or p35 G2A-Flag were detected by immunoblotting with anti-Flag antibody (top) and then quantified (bottom). Data represent the means ± the standard error ($n = 3$, $**p < 0.05$, Student's t test). (E) Rate of degradation of p39 and p39 G2A in HEK293 cells. HEK293 cells co-expressing Cdk5 and p39 or p39 G2A were treated with 10 μg/mL CHX for the indicated times. Immunoblots of p39, p39 G2A, and Cdk5 are shown in the top panel, and quantification of p39 and p39 G2A is shown in the bottom panel: (○) p39 and (●) p39 G2A. Data represent the means ± the standard error ($n = 3$, $*p < 0.05$, $**p < 0.01$, Student's t test).

of the p10 region, we expressed the p10 region-GFP fusion proteins, $N98^{p35}$-GFP and $N100^{p39}$-GFP, and compared their degradation. $N98^{p35}$-GFP was degraded faster than $N100^{p39}$-GFP (Figure S1A of the Supporting Information). Together, these results suggest that the degradation rates of p35 and p39 are determined by binding to Cdk5 and that the difference in degradation rates is conferred by their p10 regions.

Degradation of p35 and p39 by Proteasomes Is Facilitated by Association with Membranes. On the basis of the results given above that the p10 region affects the degradation rate, we hypothesized that the membrane binding via N-terminal myristoylation of the p10 region might play an important role (*16*, *20*). Thus, we examined the effect of myristoylation on the stability of p35 and p39 using mutants species thereof, in which the myristoylation sites had been disabled through substitution of Gly with Ala at amino acid position 2 (G2A) (*14*). When the G2A mutants of p35 and p39 (p35 G2A and p39 G2A) were expressed in HEK293 cells, their expression levels were significantly higher than those of WT p35 and p39, respectively (Figure 4A,B). The G2A mutation increased the percentages of p35 and p39 in the soluble fraction, although more than half of the p39 G2A was still recovered in the particulate fraction. In contrast, p35 G2A was primarily detected in the supernatant (Figure S2A,B of the Supporting Information). These results suggest that p39 might have an additional membrane binding site.

The higher protein level of G2A mutants suggests that they are more stable than the WT form. We then examined the rate of degradation of G2A mutants. The amount of p35 G2A decreased more slowly than the amount of WT p35 in the presence of CHX (Figure 4C). We also asked if the G2A mutation affected the stability of activators in neurons. Slower degradation of p35 G2A was observed in cerebellar granule neurons where p35 and its G2A mutant were exogenously expressed (Figure 4D). A similar result for degradation was observed for the G2A mutation of p39 in HEK293 cells (Figure 4E). The decrease in the protein levels of p35 G2A and p39 G2A was suppressed by Epoxomicin or MG132 (Figure S3A,B of the Supporting Information), indicating that G2A mutants are also degraded by proteasomes.

To measure the turnover rates more precisely, we performed pulse−chase experiments (Figure 5A,B). These experiments

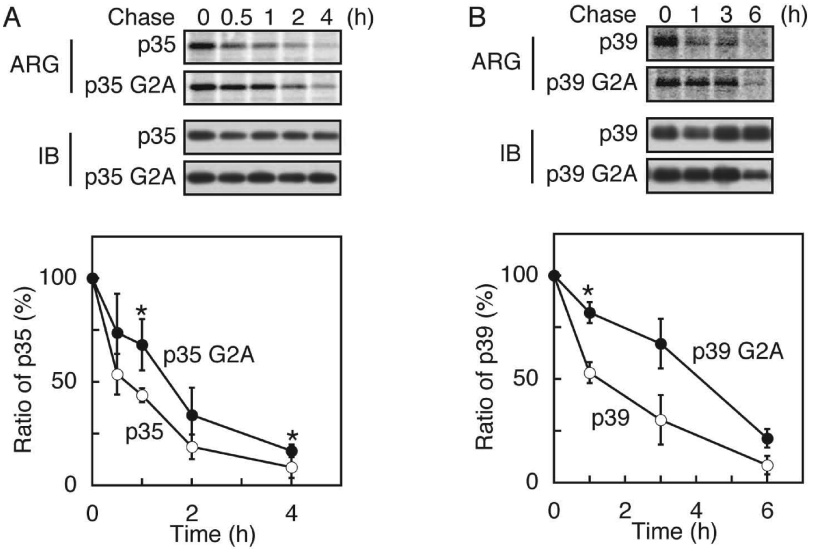

FIGURE 5: Rate of degradation of p35, p39, and their G2A mutants analyzed by pulse−chase labeling. (A) HEK293 cells co-expressing Cdk5 and p35 or p35 G2A were cultured in the presence of [^{35}S]methionine (4.07×10^6 Bq/mL) for 1 h and chased for the indicated times. p35 or p35 G2A was immunoprecipitated using an anti-p35 antibody followed by autoradiography (ARG) and immunoblotting (IB). Radioactive p35 was quantified after normalization to the amount of p35 estimated by immunoblotting (bottom): (○) p35 and (●) p35 G2A. Data represent the means ± the standard error ($n = 3$, $^*p < 0.05$, Student's t test). (B) HEK293 cells co-expressing Cdk5 and p39 or p39 G2A were treated and analyzed as described for panel A. Immunoprecipitation was performed using an anti-p39 antibody: (○) p39 and (●) p39 G2A. Data represent the means ± the standard error ($n = 3$, $^*p < 0.05$, Student's t test).

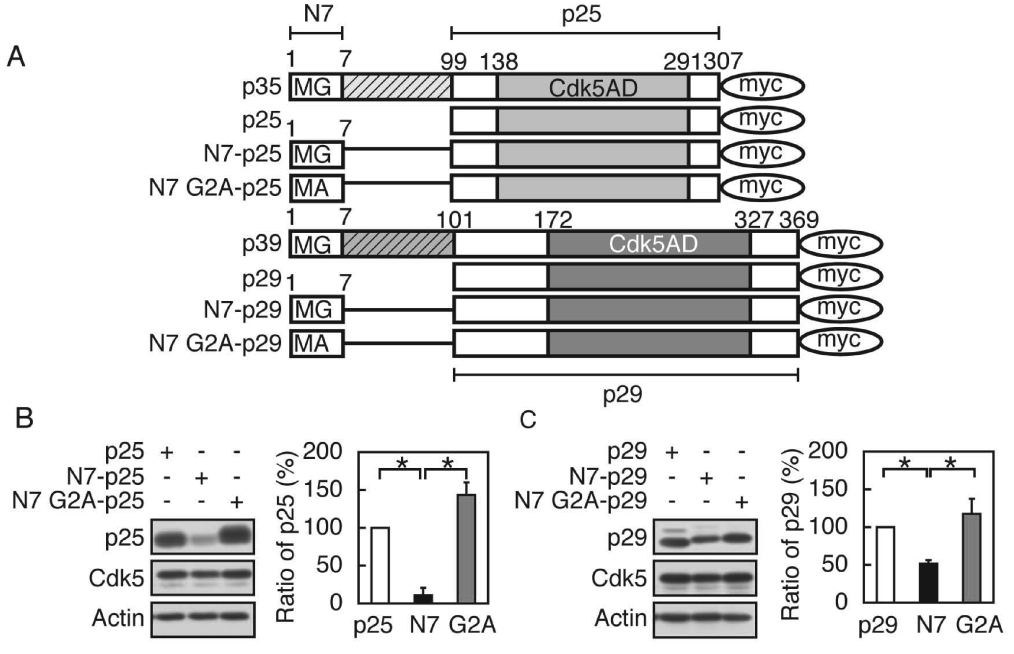

FIGURE 6: N-Terminal seven-amino acid tag including the myristoylation site alters the stability of p25 and p29. (A) Schematic representation of p35, p25, N7-p25, and N7 G2A-p25 and the corresponding constructs of p39. The first two amino acids, Met and Gly, are indicated by MG, and Ala mutants of Gly at amino acid position 2 (G2A) are shown by MA. The full length of p35 is 307 amino acids, and that of p39 is 369 amino acids. The C-terminal Cdk5 activation domains (Cdk5AD) of p35 and p39 are colored light and dark gray, respectively. (B) Expression of p25, N7-p25, or N7 G2A-p25 in HEK293 cells. HEK293 cells were cotransfected with Cdk5 and p25, N7-p25, or N7 G2A-p25 expression plasmids for 24 h followed by immunoblot analysis using an anti-p35 antibody to detect p25 constructs or an anti-Cdk5 antibody. Actin was analyzed as a loading control. The levels of N7-p25 or N7 G2A-p25 relative to that of p25 are shown in the right panel. Data represent the means ± the standard errors ($n = 3$, $^*p < 0.05$, Student's t test). (C) Expression of p29, N7-p29, or N7 G2A-p29 in HEK293 cells. HEK293 cells were cotransfected with Cdk5 and p29, N7-p29, or N7 G2A-p29 expression plasmids for 24 h followed by immunoblot analysis using an anti-myc antibody to detect p29 constructs or an anti-Cdk5 antibody. The levels of N7-p29 or N7 G2A-p29 relative to that of p29 are shown in the right panel. Data represent the means ± the standard error ($n = 3$, $^*p < 0.05$, Student's t test).

verified that both G2A mutants had slower turnover rates than their respective WT forms. Levels of p35 and p39 were decreased by 60 and 50%, respectively, as compared to 30 and 20% for p35 G2A and p39 G2A, respectively, after a 1 h chase (Figure 5A,B). Together, these results suggest that degradation of both p35 and p39 is stimulated by association with membranes via myristoylation in the N-terminal p10 region.

Degradation of p25 and p29 and Their Corresponding Membrane-Bound Forms, N7-p25 and N7-p29, Respectively. Fragments p25 and p29 are stable and exhibit slow

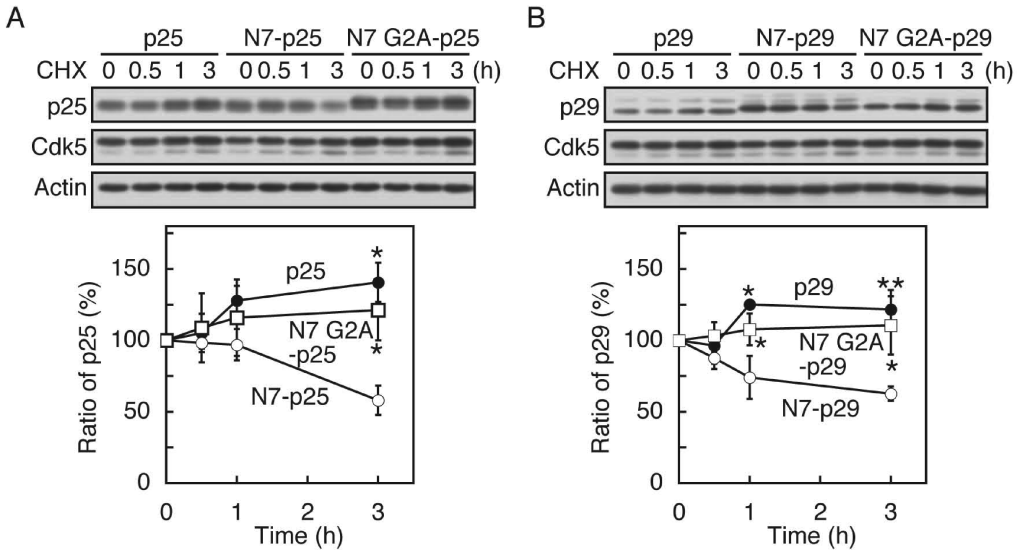

FIGURE 7: Rate of degradation of p25, p29, and the N7-tagged variants. (A) Rate of degradation of p25, N7-p25, or N7 G2A-p25 in HEK293 cells. HEK293 cells co-expressing Cdk5 and p25, N7-p25, or N7 G2A-p25 were treated with 10 μg/mL CHX for the indicated times. p25, N7-p25, or N7 G2A-p25 and Cdk5 were detected by immunoblotting using an anti-p35 antibody to detect p25 constructs or an anti-Cdk5 antibody. Actin was analyzed as a loading control. The levels of p25, N7-p25, and N7 G2A-p25 were quantified in the bottom panel: (●) p25, (○) N7-p25, and (□) N7 G2A-p25. Data represent the means ± the standard error ($n = 3$, $^*p < 0.05$, Student's t test). (B) Rate of degradation of p29, N7-p29, or N7 G2A-p29 in HEK293 cells. HEK293 cells co-expressing Cdk5 and p29, N7-p29, or N7 G2A-p29 were treated with 10 μg/mL CHX for the indicated times. p29, N7-p29, or N7 G2A-p29 and Cdk5 were detected by immunoblotting using an anti-myc (9E10) antibody to detect p29 constructs or an anti-Cdk5 antibody. Actin was analyzed as a loading control. The levels of p29, N7-p29, or N7 G2A-p29 were quantified in the bottom panel: (●) p29, (○) N7-p29, and (□) N7 G2A-p29. Data represent the means ± the standard error ($n = 3$, $^*p < 0.05$, $^{**}p < 0.01$, Student's t test).

degradation rates (*10*, *15*). However, the absence of the N-terminal p10 region or dissociation from membranes has not been shown to be responsible for the stability of p25 and p29. To assess the role of myristoylation in a manner that is independent of the p10 region, we constructed N7-p25 and N7-p29, in which p25 and p29, respectively, were tagged with the N-terminal common seven amino acids (Met-Gly-Thr-Val-Leu-Ser-Leu) of p35 and p39 (Figure 6A). We also constructed the corresponding G2A mutants, N7 G2A-p25 and N7 G2A-p29, as a reference. The solubility of the proteins is shown in Figure S2C,D of the Supporting Information. N7-p25 and N7-p29 were detected in the pellet fraction, whereas N7 G2A-p25 and N7 G2A-p29, as well as p25 and p29, were detected only in the cytosolic fraction (Figure S2C,D of the Supporting Information). We also observed the subcellular localization of these proteins using immunofluorescence staining. Expression products p25, p29, N7 G2A-p25, and N7 G2A-p29 were distributed diffusely in the cytoplasm, whereas N7-p25 and N7-p29 were localized primarily in the perinuclear region. The distribution of N7-p25 and N7-p29 was comparable to that of p35 and p39, although perinuclear accumulation was stronger for p35 and p39 (Figure S4 of the Supporting Information). These results indicate that N7-p25 and N7-p29 were bound to the perinuclear membrane organelles, similar to p35 and p39 (*16*). When they were expressed transiently in HEK293 cells, expression levels of both N7-p25 and N7-p29 were low in comparison to those of p25, p29, and the G2A mutants (Figure 6B,C). Quantification indicated that p25 or N7 G2A-p25 exhibited ~10- or ~14-fold higher protein levels than N7-p25, respectively, and p29 or N7 G2A-p29 exhibited ~2-fold higher levels than N7-p29.

After proteasome-dependent degradation of N7-p25 and N7-p29 using Epoxomicin or MG132 had been confirmed (Figure S3C,D of the Supporting Information), the degradation rates of N7-p25 and N7-p29 were compared with the corresponding G2A mutants in the presence of CHX. N7-p25 and N7-p29 were degraded by approximately 50% at 3 h, whereas p25, p29, N7 G2A-p25, and N7 G2A-p29 were stable for observation for at least 3 h (Figure 7A,B). These results suggest that membrane association via myristoylation is sufficient to diminish the half-life of p25 and p29, and that endogenous p25 becomes stable mainly by dissociation from membranes, after cleavage with calpain.

Cleavage of p35 and p39 by Calpain Is Facilitated by Association with Membranes. The Cdk5 activators, p35 and p39, are cleaved by calpain to form p25 and p29, respectively (*10*, *19*, *20*). As the cleavage of p35 and p39 in neurons has not been directly compared, we assessed the cleavage in cultured neurons by treating cells with the Ca^{2+} ionophore ionomycin to activate calpain. We used cortical neurons (Figure 8A) and cerebellar granule neurons (Figure 8B) on DIV14, cultured for periods of time longer than those used for the degradation experiments in Figure 1 because the calpain cleavage becomes predominant with a longer duration of culturing (*28*). When cortical neurons and cerebellar granule neurons in cultures on DIV14 were treated with 10 μM ionomycin and 2 mM $CaCl_2$ for 15 min, both p35 and p39 were cleaved to p25 and p29, respectively (Figure 8A,B). However, the level of p35 cleavage was higher than that of p39 in both cortical and cerebellar granule neurons (Figure 8A,B). When the calpain cleavage was compared between cortical and cerebellar granule neurons, the level of p35 cleavage was higher in cortical neurons than in cerebellar granule neurons, suggesting cell-specific differences in calpain activity.

Next, the cleavage level of p35 and p39 was analyzed under excitotoxic condition. When cortical neurons were treated with 1 mM glutamate, a concentration higher than that used in Figure 1, for 1 h, most of p35 was cleaved and a strong signal of p25 was detected. Formation of p29 was also detected, but most of the p39 remained uncleaved (Figure 8C). When cerebellar granule

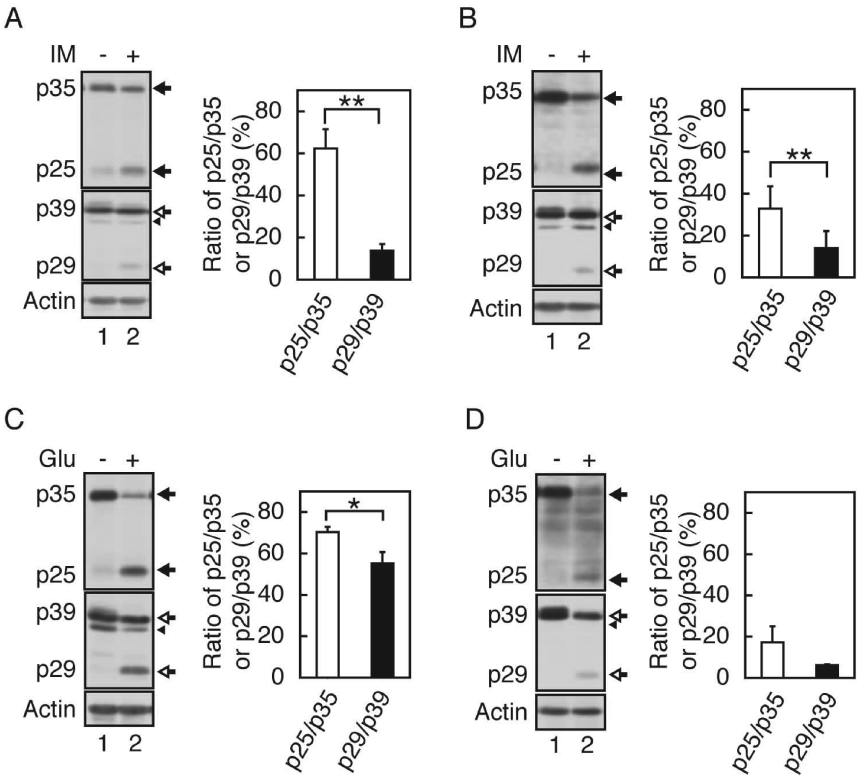

FIGURE 8: Cleavage of p35 and p39 by calpain in cultured neurons. (A) Ionomycin-induced cleavage of p35 and p39 to p25 and p29, respectively, in cortical neurons. Cerebral cortical neurons on DIV14 were treated with 10 μM ionomycin (IM) for 15 min. p35 and p25 or p39 and p29 were detected by immunoblotting using an anti-p35 or anti-p39 antibody, respectively. Actin was analyzed as a loading control. p35 or p25 and p39 or p29 are indicated by black and white arrows, respectively. The arrowhead in the p39 blot indicates a nonspecific band. The ratios of p25 (lane 2) generated from the parent p35 (lane 1) and p29 (lane 2) generated from the parent p39 (lane 1) are shown in the graph. Data represent the means ± the standard error ($n = 3$, $^{**}p < 0.01$, Student's t test). (B) Ionomycin-induced cleavage of p35 and p39 to p25 and p29, respectively, in cerebellar granule neurons. Cerebellar granule neurons on DIV14 were treated and analyzed as described for panel A. Data represent the means ± the standard error ($n = 3$, $^{**}p < 0.01$, Student's t test). (C) Glutamate-induced cleavage of p35 and p39 to p25 and p29, respectively, in cortical neurons. Cerebral cortical neurons on DIV14 were treated with 1 mM glutamate (Glu) for 1 h. p35 and p25 or p39 and p29 were detected by immunoblotting using anti-p35 or anti-p39 antibody, and the ratios of p25 (lane 2) to p35 (lane 1) and p29 (lane 2) to p39 (lane 1) were analyzed as described for panel A. Data represent the means ± the standard error ($n = 3$, $^{*}p < 0.05$, Student's t test). (D) Glutamate-induced cleavage of p35 and p39 to p25 and p29, respectively, in cerebellar granule neurons. Cerebellar granule neurons on DIV14 were treated with 1 mM glutamate (Glu) for 1 h. p35 and p25 or p39 and p29 were detected by immunoblotting using anti-p35 or anti-p39 antibody, and the ratios of p25 (lane 2) to p35 (lane 1) and p29 (lane 2) to p39 (lane 1) were analyzed as described in panel A. Data represent the means ± the standard error ($n = 3$, Student's t test). No significant difference was observed in panel D.

neurons were treated, p25 was detected but the amount of p25 generated was smaller than that in cortical neurons. The level of formation of p29 was low in cerebellar granule neurons treated with glutamate, in fact much lower than that in cortical neurons. Together, these results reveal that p35 is more prone to excitotoxic-induced cleavage. Moreover, different types of neurons seem to display different degrees of calpain-dependent cleavage. For example, cerebellar granule neurons show only a low level of cleavage as compared to cortical neurons.

We also investigated the effect of membrane association on calpain-mediated cleavage using the G2A mutants of p35 and p39. When HEK293 cells expressing p35 or p39 were treated with ionomycin for 1 h, p25 or p29 was detected, but only a lesser degree of cleavage occurred compared to that in cortical neurons, consistent with a previous report (*30*). Cleavage of p35 G2A and p39 G2A in HEK293 cells was assessed by immunoblots with long exposure times (Figure 9, second panel labeled "long"). p35 G2A and p39 G2A were cleaved to p25 and p29, respectively, but to a lesser extent than their WT forms (Figure 9). When the amount of p25 and p29 generated was quantitatively measured, the amount of cleavage product from the G2A mutants was approximately half of that from WT p35 and p39. These results indicate that the cleavage of p35 and p39 by calpain is also enhanced by association with membranes, as observed for their proteasomal degradation. However, p35 and p39 showed distinct levels of cleavage, and thus, it is likely that they induce aberrant Cdk5 activation differently. Moreover, the difference in p35 and p39 cleavage between cortical neurons and cerebellar granule neurons suggests that aberrant activation of Cdk5 seems to be regulated in a cell type-specific manner.

DISCUSSION

The kinase activity of Cdk5 is determined by the available amount of p35 or p39. The molecular mechanisms determining the amount of p35 and p39 are critical for understanding Cdk5 functions; however, currently, the processes are not well understood, and only a few reports have tried to address this question. In our study, we have focused on the mechanisms that confer degradation of p35 and p39 in neurons. We found that both p35 and p39 were degraded by proteasomes in cultured neurons but that the degradation rate was lower for p39 than p35. The N-terminal p10 region determined the proteolytic properties of p35 and p39. In addition, we showed that not only the degradation

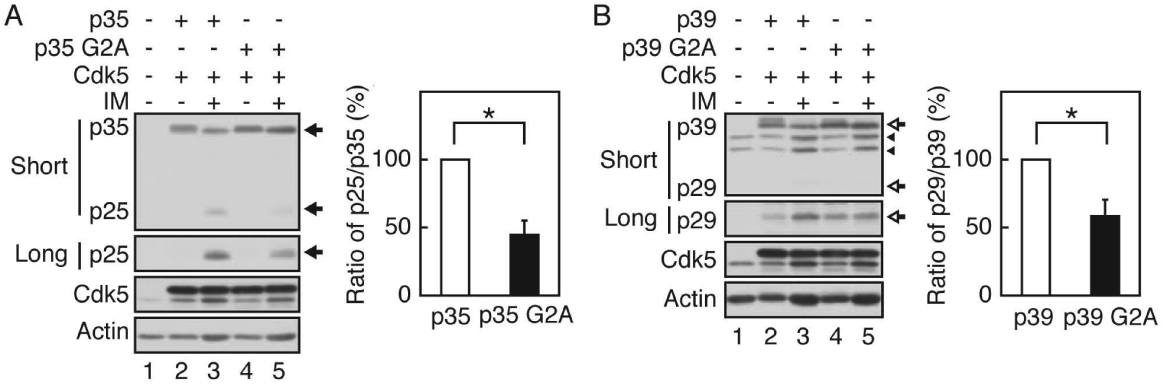

FIGURE 9: Cleavage of p35, p39, and their G2A mutants by calpain. (A) Cleavage of p35 or p35 G2A in HEK293 cells. HEK293 cells co-expressing Cdk5 and p35 or p35 G2A were treated with 20 μM ionomycin for 30 min. p35 or p35 G2A and Cdk5 were detected by immunoblotting using anti-p35 and anti-Cdk5 antibodies, respectively. Long exposure of the p25 blot is shown in the second panel. p35 and p25 are denoted with black arrows. The ratio of p25 (lane 3 or 5 in the long exposure panel) to p35 (lane 2) or p35 G2A (lane 4) was calculated and is expressed as a percentage of the ratio of p25 (lane 3 or 5 in the long exposure panel) to p35 (lane 2) or p35 G2A (lane 4) (right panel). Data represent the means $\pm$ the standard error ($n = 3$, $^*p < 0.05$, Student's t test). (B) Cleavage of p39 or p39 G2A in HEK293 cells. HEK293 cells co-expressing Cdk5 and p39 or p39 G2A were treated with 20 μM ionomycin for 30 min. p39 or p39 G2A and Cdk5 were detected by immunoblotting with anti-p39 and anti-Cdk5 antibodies, respectively. A long exposure of the p29 blot is shown in the second panel. p39 and p29 are denoted with white arrows. Arrowheads denote nonspecific bands. The ratio of p29 (lane 3 or 5 in the long exposure panel) to p39 (lane 2) or p39 G2A (lane 4) was calculated and is expressed as a percentage of the ratio of p29 (lane 3 or 5 in the long exposure panel) to p39 (lane 2) or p39 G2A (lane 4) (right panel). Data represent the means $\pm$ the standard error ($n = 3$, $^*p < 0.05$, Student's t test).

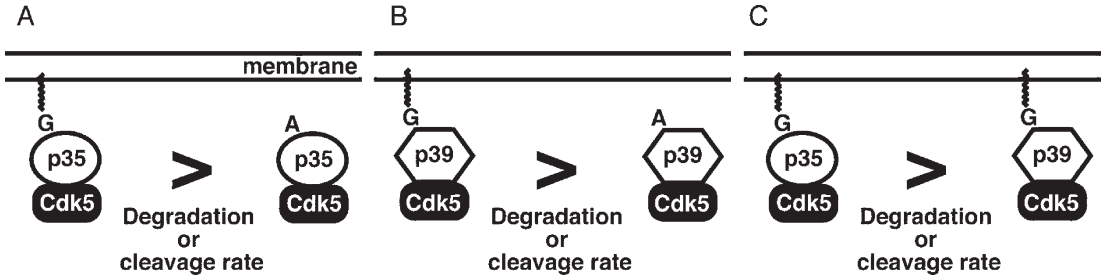

FIGURE 10: Degradation or cleavage rates of p35 and p39. Cdk5-p35 and Cdk5-p39 associate with membranes via myristoylation at the N-terminal Gly of p35 and p39, respecdtively. (A and B) Ala mutation at the myristoylation site of p35 (A) and p39 (B) reduced the degradation and cleavage rates, indicating that membrane association facilitates the degradation and cleavage of both p35 and p39. (C) Proteasomal degradation and cleavage by calpain are more rapid for p35 than for p39.

of p35 and p39 by proteasomes but also the cleavage by calpain was facilitated by association with membranes. We demonstrate that the dynamic metabolism of p35 and p39 (and hence the physiological regulation and abnormal activation of the Cdk5 activity) occurs in the vicinity of membranes in the cytoplasm of neurons.

p35 is known to have a short half-life, which is regulated by proteasomal degradation (*8*, *9*). However, it is not known where in cells p35 is degraded and what factors determine the lifetime. In contrast to p35, p25 is a more stable fragment with a long half-life (*15*). Removal of the N-terminal p10 region makes p25 stable but also causes dissociation from membranes (*15*). It was not known whether removal of the p10 region or the resulting dissociation from membranes was responsible for the stability of p25. We have shown that the G2A mutation was sufficient to stabilize p35 (Figure 10A). Furthermore, p25 became unstable when it was tagged with the seven N-terminal amino acids including the myristoylation site. These results clearly indicate that membrane association is an important factor affecting degradation of p35. N7-p25, which is lacking the majority of the p10 region, was degraded more slowly than p35, suggesting that parts of the p10 region also affect p35 degradation. Accordingly, the p10 region constitutes the basic region with an isoelectric point of 10.7, which has been shown to be involved in membrane binding. Together, our results propose that myristoylation and the basic region act cooperatively to localize p35 to membranes and thereby increase the rate of turnover of p35.

Proteins with a short half-life, such as p35, are commonly degraded via the ubiquitin proteasome pathway. This pathway requires the tagging of proteins with ubiquitin by E3 ligases prior to degradation, and as such, E3 ligases have been shown to colocalize with target proteins. For example, cyclins, which are Cdk activators regulating cell cycle processes, are localized in the nucleus along with E3 ligase in proliferating cells (*31*−*35*). Although E3 ligase of p35 has not been demonstrated in neurons, it is likely that E3 ligase for p35 is associated with membranes to regulate Cdk5 activity through degradation of p35.

p35 is cleaved to p25 by calpain (*19*, *20*), which induces aberrant activation of Cdk5 (*20*), mislocalization into the cytoplasm or nucleus (*15*, *16*, *36*, *37*), and release from the inhibitory effect of membranes (*21*). We have shown here that formation of p25 is facilitated by association of p35 with membranes (Figure 10A). This is consistent with the known activation process of calpain (*38*). Inactive calpain is a soluble cytoplasmic protein. An increased intracellular level of Ca^{2+} activates calpain via N-terminal truncation. Upon activation, calpain is translocated to membranes by an as yet unknown mechanism, resulting

in preferential cleavage of membrane-bound proteins (*39*, *40*). Spectrin, which is a widely used marker of calpain activation, is a typical example of a membrane-localized protein that undergoes calpain cleavage. Similarly, membrane-bound p35 may also be a good substrate for calpain.

p25−Cdk5 is generated in neurons undergoing cell death, and this complex has been implicated in the neuronal cell death processes (*15*, *36*, *37*). Abnormal activation of Cdk5 by calpain-dependent cleavage of p35 to generate p25 has been associated with neurodegenerative diseases such as Alzheimer's disease (AD) (*15*, *19*, *20*). Interestingly, the extent of cleavage of p35 is lower in cerebellar granule neurons than in cortical neurons. The cerebellum is much less affected pathologically compared to cortical regions in AD (*41*−*43*). In the cerebellum, a decreased level of p25 generation can be explained by the high level of expression of calpastatin, an endogenous calpain inhibitor protein (*44*). As yet, there is no direct evidence supporting a relationship between high levels of calpastatin and a lack of AD pathology in cerebellum (for a discussion, see refs (*44*−*46*)). Nevertheless, a decreased level of p25 generation in the cerebellum may give further support for such an involvement.

At present, only one report has described the degradation and cleavage of p39 (*10*). This study analyzed the cleavage of endogenous p39 in brains or cultured neurons and degradation of exogenously expressed p39 in COS-7 cells. We confirmed the cleavage of p39 to p29 in neurons treated with excitotoxic glutamate. Our results for the degradation of p39 using cultured neurons are in agreement with the observations in COS-7 cells. Furthermore, our study demonstrates that p35, as well as p39, is degraded by proteasomes or cleaved by calpain when localized in the proximity of membranes (Figure 10C). Even though proteolysis of p39 seems to be regulated in a manner similar to that of p35, some quantitative differences in the degradation of p35 and p39 were observed. Proteasomal degradation of p39 reached a level of approximately 50% after 6 h in cerebellar granule neurons, which is several times lower than the degradation rate of p35. The degradation rate can be affected by several properties of a degrading protein such as the presence of a degradation motif in the primary sequence, a degradation signal tagged by phosphorylation, and cellular localization (*47*−*49*). We screened p35 and p39 for various degradation motifs, including that commonly found in cyclins, but could not conclusively demonstrate any. What factors regulate the degradation of p35 and p39, and what distinguishes their degradation rates? The amino acid sequences of p35 and p39 are 57% identical, with a particularly high level of identity (72%) in the Cdk5 binding region. Considering that p25 and p29 are relatively stable proteins, a putative degradation motif is likely to be present in the N-terminal p10 region. This was confirmed by experiments in which the cognate p10 regions were swapped between p35 and p39 which demonstrate that it is the N-terminal p10 region that determines the degradation rate of the chimeric proteins.

A known degradation signal for p35 is phosphorylation (*8*, *9*, *28*). Phosphorylation by Cdk5 stimulates degradation of p35 in neurons and HEK293 cells. The Cdk5 phosphorylation sites are Ser8 and Thr138. Of these two sites, Thr138 is suggested to be the one recognized for ubiquitination by E3 ligase (*8*, *30*). p39 is also phosphorylated by Cdk5 (*18*), and the sites corresponding to those of p35 appear to be phosphorylated (A. Asada et al., unpublished results). However, it is has not been determined whether this phosphorylation functions as a signal for the degradation of p39. If the phosphorylation is the degradation signal as well for p39, the slower degradation rate could be explained by weaker phosphorylation of p39, resulting from the lower binding affinity of p39 for Cdk5 (*18*).

Mice lacking p39 display no apparent phenotype, whereas knockout or knockdown of p35 results in defects in neuronal migration, synapse formation, and synaptic activity (*12*, *23*−*25*, *50*, *51*). At present, physiological functions of p39−Cdk5 are not known. Previously characterized heterogeneity in biochemical properties between p35 and p39 includes different spatiotemporal patterns of protein synthesis and the stability of the complex with Cdk5 (*18*, *29*). While the expression of p35 commences in embryonic neurons, the expression of p39 starts mostly after embryonic brain development, especially in the cerebral cortex (*29*). p39 and Cdk5 dissociate in the presence of nonionic detergent, whereas p35−Cdk5 is stable and activated (*18*). These results have elucidated other differences between the two activators, including differences in half-lives and calpain cleavage. The different rates of glutamate-induced degradation may be associated with the differential function in synaptic activity between p35 and p39. p35 is quickly degraded after glutamate application, suggesting a role for p35−Cdk5 in acute synaptic responses. Slower degradation of p39 may reflect its function in slower neuronal responses or participation in housekeeping processes in mature neurons. Slower cleavage of p39 may also point to a less significant contribution to neurodegenerative diseases.

ACKNOWLEDGMENT

This paper is dedicated to the late Shinya Miyauchi, a valued member of our laboratory. We thank Drs. Florian Plattner and Marco Angelo at University College London (London, U.K.) for proofreading the manuscript.

SUPPORTING INFORMATION AVAILABLE

Subcellular localization of p35, p35 G2A, p39, or p39 G2A characterized by cell fractionation experiments and subcellular localization of p25, N7-p25, N7 G2A-p25, p29, N7-p29, and N7 G2A-p29 examined by cell fractionation and immunofluorescence staining. This material is available free of charge via the Internet at http://pubs.acs.org.

REFERENCES

1. Dhavan, R., and Tsai, L. H. (2001) A decade of CDK5. *Nat. Rev. Mol. Cell Biol. 2*, 749–759.
2. Shelton, S. B., and Johnson, G. V. W. (2004) Cyclin-dependent kinase-5 in neurodegeneration. *J. Neurochem. 88*, 1313–1326.
3. Cheung, Z. H., Fu, A. K., and Ip, N. Y. (2006) Synaptic roles of Cdk5: Implications in higher cognitive functions and neurodegenerative diseases. *Neuron 50*, 13–18.
4. Angelo, M., Plattner, F., and Giese, K. P. (2006) Cyclin-dependent kinase 5 in synaptic plasticity, learning and memory. *J. Neurochem. 99*, 353–370.
5. Tang, D., and Wang, J. H. (1996) Cyclin-dependent kinase 5 (Cdk5) and neuron-specific Cdk5 activators. *Prog. Cell Cycle Res. 2*, 205–216.
6. Hisanaga, S., and Saito, T. (2003) The regulation of cyclin-dependent kinase 5 activity through the metabolism of p35 or p39 Cdk5 activator. *Neurosignals 12*, 221–229.
7. Qi, Z., Huang, Q. Q., Lee, K. Y., Lew, J., and Wang, J. H. (1995) Reconstitution of neuronal Cdc2-like kinase from bacteria-expressed Cdk5 and an active fragment of the brain-specific activator. Kinase activation in the absence of Cdk5 phosphorylation. *J. Biol. Chem. 270*, 10847–10854.
8. Patrick, G. N., Zhou, P., Kwon, Y. T., Howley, P. M., and Tsai, L. H. (1998) p35, the neuronal-specific activator of cyclin-dependent kinase 5 (Cdk5) is degraded by the ubiquitin-proteasome pathway. *J. Biol. Chem. 273*, 24057–24064.

9. Saito, T., Ishiguro, K., Onuki, R., Nagai, Y., Kishimoto, T., and Hisanaga, S. (1998) Okadaic acid-stimulated degradation of p35, an activator of CDK5, by proteasome in cultured neurons. *Biochem. Biophys. Res. Commun. 252*, 775–778.
10. Patzke, H., and Tsai, L. H. (2002) Calpain-mediated cleavage of the cyclin-dependent kinase-5 activator p39 to p29. *J. Biol. Chem. 277*, 8054–8060.
11. Morgan, D. O. (1997) Cyclin-dependent kinases: Engines, clocks, and microprocessors. *Annu. Rev. Cell Dev. Biol. 13*, 261–291.
12. Wei, F. Y., Tomizawa, K., Ohshima, T., Asada, A., Saito, T., Nguyen, C., Bibb, J. A., Ishiguro, K., Kulkarni, A. B., Pant, H. C., Mikoshiba, K., Matsui, H., and Hisanaga, S. (2005) Control of cyclin-dependent kinase 5 (Cdk5) activity by glutamatergic regulation of p35 stability. *J. Neurochem. 93*, 502–512.
13. Hosokawa, T., Saito, T., Asada, A., Ohshima, T., Itakura, M., Takahashi, M., Fukunaga, K., and Hisanaga, S. (2006) Enhanced activation of Ca^{2+}/calmodulin-dependent protein kinase II upon downregulation of cyclin-dependent kinase 5-p35. *J. Neurosci. Res. 84*, 747–754.
14. Boutin, J. A. (1997) Myristoylation. *Cell. Signalling 9*, 15–35.
15. Patrick, G. N., Zukerberg, L., Nikolic, M., de la Monte, S., Dikkes, P., and Tsai, L. H. (1999) Conversion of p35 to p25 deregulates Cdk5 activity and promotes neurodegeneration. *Nature 402*, 615–622.
16. Asada, A., Yamamoto, N., Gohda, M., Saito, T., Hayashi, N., and Hisanaga, S. (2008) Myristoylation of p39 and p35 is a determinant of cytoplasmic or nuclear localization of active cyclin-dependent kinase 5 complexes. *J. Neurochem. 106*, 1325–1336.
17. Tarricone, C., Dhavan, R., Peng, J., Areces, L. B., Tsai, L. H., and Musacchio, A. (2001) Structure and regulation of the CDK5-p25-(nck5a) complex. *Mol. Cell 8*, 657–669.
18. Yamada, M., Saito, T., Sato, Y., Kawai, Y., Sekigawa, A., Hamazumi, Y., Asada, A., Wada, M., Doi, H., and Hisanaga, S. (2007) Cdk5−p39 is a labile complex with the similar substrate specificity to Cdk5−p35. *J. Neurochem. 102*, 1477–1487.
19. Kusakawa, G., Saito, T., Onuki, R., Ishiguro, K., Kishimoto, T., and Hisanaga, S. (2000) Calpain-dependent proteolytic cleavage of the p35 cyclin-dependent kinase 5 activator to p25. *J. Biol. Chem. 275*, 17166–17172.
20. Lee, M. S., Kwon, Y. T., Li, M., Peng, J., Friedlander, R. M., and Tsai, L. H. (2000) Neurotoxicity induces cleavage of p35 to p25 by calpain. *Nature 405*, 360–364.
21. Patzke, H., Maddineni, U., Ayala, R., Morabito, M., Volker, J., Dikkes, P., Ahlijanian, M. K., and Tsai, L. H. (2003) Partial rescue of the p35−/− brain phenotype by low expression of a neuronal-specific enolase p25 transgene. *J. Neurosci. 23*, 2769–2778.
22. Zhu, Y. S., Saito, T., Asada, A., Maekawa, S., and Hisanaga, S. (2005) Activation of latent cyclin-dependent kinase 5 (Cdk5)-p35 complexes by membrane dissociation. *J. Neurochem. 94*, 1535–1545.
23. Chae, T., Kwon, Y. T., Bronson, R., Dikkes, P., Li, E., and Tsai, L. H. (1997) Mice lacking p35, a neuronal specific activator of Cdk5, display cortical lamination defects, seizures, and adult lethality. *Neuron 18*, 29–42.
24. Ko, J., Humbert, S., Bronson, R. T., Takahashi, S., Kulkarni, A. B., Li, E., and Tsai, L. H. (2001) p35 and p39 are essential for cyclin-dependent kinase 5 function during neurodevelopment. *J. Neurosci. 21*, 6758–6771.
25. Ohshima, T., Ward, J. M., Huh, C. G., Longenecker, G., Veeranna, Pant, H. C., Brady, R. O., Martin, L. J., and Kulkarni, A. B. (1996) Targeted disruption of the cyclin-dependent kinase 5 gene results in abnormal corticogenesis, neuronal pathology and perinatal death. *Proc. Natl. Acad. Sci. U.S.A. 93*, 11173–11178.
26. Tabuchi, A., Oh, E., Taoka, A., Sakurai, H., Tsuchiya, T., and Tsuda, M. (1996) Rapid attenuation of AP-1 transcriptional factors associated with nitric oxide (NO)-mediated neuronal cell death. *J. Biol. Chem. 271*, 31061–31067.
27. Endo, R., Saito, T., Asada, A., Kawahara, H., Ohshima, T., and Hisanaga, S. (2009) Commitment of 1-methyl-4-phenylpyrinidinium ion-induced neuronal cell death by proteasome-mediated degradation of p35 cyclin-dependent kinase 5 activator. *J. Biol. Chem. 284*, 26029–26039.
28. Saito, T., Onuki, R., Fujita, Y., Kusakawa, G., Ishiguro, K., Bibb, J. A., Kishimoto, T., and Hisanaga, S. (2003) Developmental regulation of the proteolysis of the p35 cyclin-dependent kinase 5 activator by phosphorylation. *J. Neurosci. 23*, 1189–1197.
29. Takahashi, S., Saito, T., Hisanaga, S., Pant, H. C., and Kulkarni, A. B. (2003) Tau phosphorylation by cyclin-dependent kinase 5/p39 during brain development reduces its affinity for microtubules. *J. Biol. Chem. 278*, 10506–10515.
30. Kamei, H., Saito, T., Ozawa, M., Fujita, Y., Asada, A., Bibb, J. A., Saido, T. C., Sorimachi, H., and Hisanaga, S. (2007) Suppression of calpain-dependent cleavage of the CDK5 activator p35 to p25 by site-specific phosphorylation. *J. Biol. Chem. 282*, 1687–1694.
31. Obaya, A. J., and Sedivy, J. M. (2002) Regulation of cyclin-Cdk activity in mammalian cells. *Cell. Mol. Life Sci. 59*, 126–142.
32. Moroy, T., and Geisen, C. (2004) Cyclin E. *Int. J. Biochem. Cell Biol. 36*, 1424–1439.
33. Lin, D. I., Barbash, O., Kumar, K. G., Weber, J. D., Harper, J. W., Klein-Szanto, A. J., Rustgi, A., Fuchs, S. Y., and Diehl, J. A. (2006) Phosphorylation-dependent ubiquitination of cyclin D1 by the SCF (FBX4-αB Crystallin) complex. *Mol. Cell 24*, 355–366.
34. Sakaue-Sawano, A., Ohtawa, K., Hama, H., Kawano, M., Ogawa, M., and Miyawaki, A. (2008) Tracing the silhouette of individual cells in S/G2/M phases with fluorescence. *Chem. Biol. 15*, 1243–1248.
35. Lin, H. K., Wang, G., Chen, Z., Teruya-Feldstein, J., Liu, Y., Chan, C. H., Yang, W. L., Erdjument-Bromage, H., Nakayama, K. I., Nimer, S., Tempst, P., and Pandolfi, P. P. (2009) Phosphorylation-dependent regulation of cytosolic localization and oncogenic function of Skp2 by Akt/PKB. *Nat. Cell Biol. 11*, 420–432.
36. Gong, X., Tang, X., Wiedmann, M., Wang, X., Peng, J., Zheng, D., Blair, L. A., Marshall, J., and Mao, Z. (2003) Cdk5-mediated inhibition of the protective effects of transcription factor MEF2 in neurotoxicity-induced apoptosis. *Neuron 38*, 33–46.
37. Saito, T., Konno, T., Hosokawa, T., Asada, A., Ishiguro, K., and Hisanaga, S. (2007) p25/cyclin-dependent kinase 5 promotes the progression of cell death in nucleus of endoplasmic reticulum-stressed neurons. *J. Neurochem. 102*, 133–140.
38. Suzuki, K., Hata, S., Kawabata, Y., and Sorimachi, H. (2004) Structure, activation, and biology of calpain. *Diabetes 53*, S12–S18.
39. Tomimatsu, Y., Idemoto, S., Moriguchi, S., Watanabe, S., and Nakanishi, H. (2002) Proteases involved in long-term potentiation. *Life Sci. 72*, 355–361.
40. Maki, M., Kitaura, Y., Satoh, H., Ohkouchi, S., and Shibata, H. (2002) Structures, functions and molecular evolution of the penta-EF-hand Ca^{2+}-binding proteins. *Biochim. Biophys. Acta 1600*, 51–60.
41. Selkoe, D. J. (2001) Alzheimer's disease: Genes, proteins, and therapy. *Physiol. Rev. 81*, 741–766.
42. Wu, X., Jiang, X., Marini, A. M., and Lipsky, R. H. (2005) Delineating and understanding cerebellar neuroprotective pathways: Potential implication for protecting the cortex. *Ann. N.Y. Acad. Sci. 1053*, 39–47.
43. Kepe, V., Huang, S. C., Small, G. W., and Barrio, J. R. (2006) Visualizing pathology deposits in the living brain of patients with Alzheimer's disease. *Methods Enzymol. 412*, 144–160.
44. Vaisid, T., Kosower, N. S., Katzav, A., Chapman, J., and Barnoy, S. (2007) Calpastatin levels affect calpain activation and calpain proteolytic activity in APP transgenic mouse model of Alzheimer's disease. *Neurochem. Int. 51*, 391–397.
45. Nakayama, J., Yoshizawa, T., Yamamoto, N., and Arinami, T. (2002) Mutation analysis of the calpastatin gene (CAST) in patients with Alzheimer's disease. *Neurosci. Lett. 320*, 77–80.
46. Higuchi, M., Tomioka, M., Takano, J., Shirotani, K., Iwata, N., Masumoto, H., Maki, M., Itohara, S., and Saido, T. C. (2005) Distinct mechanistic roles of calpain and caspase activation in neurodegeneration as revealed in mice overexpressing their specific inhibitors. *J. Biol. Chem. 280*, 15229–15237.
47. Ho, M. A., Ou, C., Chan, Y. R., Chein, C. T., and Pi, H. (2008) The utility F-box for protein destruction. *Cell. Mol. Life Sci. 65*, 1977–2000.
48. Hunter, T. (2007) The Age of Crosstalk: Phosphorylation, Ubiquitination, and Beyond. *Mol. Cell 28*, 730–738.
49. d'Azzo, A., Bongiovanni, A., and Nastasi, T. (2005) E3 ubiqutin ligases as regulators of membrane protein trafficking and degrdation. *Traffic 6*, 429–441.
50. Ohshima, T., Ogura, H., Tomizawa, K., Hayashi, K., Suzuki, H., Saito, T., Kamei, H., Nishi, A., Bibb, J. A., Hisanaga, S., Matsui, H., and Mikoshiba, K. (2005) Impairment of hippocampal long-term depression and defective spatial learning and memory in p35 mice. *J. Neurochem. 94*, 917–925.
51. Fu, A. K., Fu, W. Y., Ng, A. K., Chien, W. W., Ng, Y. P., Wang, J. H., and Ip, N. Y. (2004) Cyclin-dependent kinase 5 phosphorylates signal transducer and activator of transcription 3 and regulates its transcriptional activity. *Proc. Natl. Acad. Sci. U.S.A. 101*, 6728–6733.